Two-photon double ionization of atoms in attosecond x-ray radiation fields

Ochbadrakh Chuluunbaatar
Joint Institute for Nuclear Research, Dubna, Moscow region 141980, Russia

Henri Bachau*
Centre des Lasers Intenses et Applications, Université Bordeaux I, Centre National de la Recherche Scientifique, Commissariat à l'Energie Atomique, 33405 Talence Cedex, France

Yuri V. Popov†
Nuclear Physics Institute, Moscow State University, Moscow 119991, Russia

Bernard Piraux‡
Institute of Condensed Matter and Nanosciences, Université Catholique de Louvain, B-1348 Louvain-la Neuve, Belgium

Kamila Stefańska
Department of Theoretical Physics and Quantum Informatics, Faculty of Applied Physics and Mathematics, Gdansk University of Technology, PL-80-952 Gdansk, Poland

(Received 30 March 2010; published 28 June 2010)

We consider two-photon double ionization of helium with 100, 200, and 400 eV excess energy for the two ejected electrons, corresponding to photon energies of 89.5, 139.5, and 239.5 eV, respectively. We focus on the case of ultrashort pulses (two oscillations of the field) and develop an approach to calculate the two-photon transition matrix elements within the lowest order of the time-dependent perturbation theory. One of the major difficulties in calculating such amplitudes is the infinite summation over a complete set of intermediate states. In the subfemtosecond regime, however, this summation can be performed accurately by means of the closure approximation. This results in a simple expression for the two-photon amplitude that contains a dipole term and a quadrupole term. The dipole term can be clearly associated to a process in which each electron absorbs a photon whereas the quadrupole term is associated to a process in which one electron absorbs two photons and ejects the second one by collision. We analyze in detail how the relative weight of both processes influences the behavior of the electron energy and angular distributions. In particular we study how the shape of these distributions changes with the amount of electron correlations taken into account in both initial and final states. For 100 eV excess energy, our results for the electron energy distribution are compared with those obtained by solving the time-dependent Schrödinger equation. All these results unveil the crucial role of electron correlations in this transient regime of ionization which is neither sequential nor direct.

DOI: 10.1103/PhysRevA.81.063424 PACS number(s): 32.80.Fb, 31.15.ve, 32.80.Rm

I. INTRODUCTION

Multiple ionization of atoms or molecules by projectiles of high energy (electrons, ions, or photons) is, in many cases, far from being well understood in spite of numerous theoretical and experimental investigations. For example, let us consider the collision of fast electrons with heavy atoms (Ne, Ar, Kr), which is characterized by a small transfer of energy and momentum from the projectile to the target electrons. At first glance, multiple ionization should be described by successive ionizations of bound electrons (the so-called ladder process, or independent ionization process); however, this is not the case. The comparison of calculations based on the model of the ladder process for the n-electron ionization total cross section [1] with experimental results [2] shows that the simple first Born approximation (Bethe formula [3]) seems sufficient to describe multiple electron release [1]. Yet the mechanism of 2,3,4, ... electron ejection following the emission of a first slow electron after a direct collision of the projectile with the target electron is not clear. A theoretical analysis of the matrix element requires the calculation of $n > 2$ electron continuum wave functions; this problem is not properly solved (see, for example, [4]).

Analogous difficulties exist in the multiphoton multiple ionization of atomic targets. Suppose that the energy of one photon is not enough for an electron to reach the ionization threshold. To escape, an electron has to absorb successively a few photons according to the energy conservation law. Again, simple arguments suggest the theoretical calculations should be based on the model of independent (sequential) absorptions. In recent experiments, where Xe atoms were interacting with xuv photons of 93 eV, Xe^{21+} ions were observed [5]. The corresponding calculations of Makris *et al.* [6] show that sequential absorption of photons does not describe the experimental results well. Even the "simple case" of two-photon double ionization (TPDI) is presently the subject of intense debate. Indeed, significant discrepancies between various theoretical

*bachau@celia.u-bordeaux1.fr
†popov@srd.sinp.msu.ru
‡bernard.piraux@uclouvain.be

results exist and the few experimental results that are available are not accurate enough to draw clear conclusions about the validity of the different theoretical approaches [7]. It is therefore necessary to pursue these investigations, on both experimental and theoretical sides.

With the development of xuv free-electron pulsed laser sources like the Linac coherent light source (SLAC National Accelerator Laboratory) [8] and x-ray free-electron laser (Deutsches Elektronen-Synchrotron) [9], the production of dense photon fluxes with photon energies close to a few keV will soon be available. High-order harmonic generation from surfaces may also provide attosecond or even zeptosecond [10] pulses, allowing extremely high intensities to be reached [11]. In this context, the study of multiphoton processes involving more than one electron has emerged as a major research field in the community. As a result, the question of multiple ionization of simple atoms or more complex structures in xuv fields has received considerable attention these last years, particularly related to experiments performed around the laser source FLASH (i.e., the free-electron laser at Hamburg). One interesting aspect of these sources is the generation of pulses or pulse trains in the femtosecond and subfemtosecond domains, opening the route to explore dynamical effects at the time scale of electron correlations. The aim of this paper is to pursue our investigations of TPDI in the xuv domain at the attosecond time scale.

First, let us recall that two mechanisms exist for TPDI; direct double ionization (DI) and sequential double ionization (SI). If we consider a laser field with an average photon energy of ω_0, a double ionization threshold $E_{\rm DI}$ for the atom A and a single ionization threshold $E_{\rm SI}$ for its parent ion A^+, direct ionization occurs for $E_{\rm DI}/2 < \omega_0 < E_{\rm SI}$. For helium, $E_{\rm DI} = 79$ eV (2.903 a.u.) and $E_{\rm SI} = 54.42$ eV (2 a.u.). For $\omega_0 > E_{\rm SI}$, sequential ionization dominates over direct ionization [12]; that is, He absorbs one photon, then a second photon ionizes the residual ion He^+. Note that, in contrast with DI, SI does not require correlations. It is important to stress that the distinction between direct and sequential transitions is only valid for long pulses. For ultrashort pulses like those considered here, the concepts of sequential and direct double ionization lose their pertinence [13]. Until now we have mainly focused on the vuv photon energy domain (40–60 eV in the helium case). In a recent publication [14], we have shown that TPDI can be expressed in a very simple form for ultrashort pulses. We focused on an average photon energy of 50 eV (i.e., just below the threshold for sequential TPDI). In this contribution, we examine the case of much higher photon energies (i.e., a regime of TPDI where a single photon has enough energy to doubly ionize the atom).

This paper is organized as follows. In Sec. II, we recall and discuss briefly the basic formulas for the calculation of the TPDI amplitude within the lowest order of the time-dependent perturbation theory. Then we examine different approximations related to the ultrashort durations of the pulses, focusing our discussion on the treatment of the electron interactions. A simple expression of the TPDI amplitude is proposed that involves direct couplings between the initial and final states. The physical meaning of this simple expression is discussed in detail. In Sec. III, we calculate the TPDI amplitude for various approximations of the initial and final states. Finally, Sec. IV is devoted to the angular and energy distributions that are calculated for photon energies of 3.29 a.u. (89.5 eV), 5.13 a.u. (139.5 eV), and 8.8 a.u. (239.5 eV), corresponding to excess energies of 100, 200, and 400 eV, respectively. The laser has few oscillations, so the pulse duration is shorter than 100 as. The results are discussed as a function of the approximation used for the initial and final states and are compared with distributions extracted from the time-dependent Schrödinger equation (TDSE). We conclude in Sec. V. Atomic units are used throughout unless otherwise stated.

II. THEORY

The two-photon transition matrix element calculated by means of the second order of the time-dependent perturbation theory in the length gauge may be written as follows [15]:

$$A_{fi}^{(2)} = \mathcal{E}_0^2 \left(\frac{1}{i}\right)^2 \int_{-\infty}^{\infty} d\tau_2 \int_{-\infty}^{\infty} d\tau_1 F(\tau_2) e^{iE_f\tau_2} \theta(\tau_2-\tau_1) \times F(\tau_1) e^{-iE_i\tau_1} \langle f|D_L e^{-i(\tau_2-\tau_1)H} D_L|i\rangle, \quad (1)$$

where $\mathcal{E}_0$ is the field amplitude and

$$D_L = \vec{e}\cdot(\vec{r}_1+\vec{r}_2),$$

where $\vec{e}$ is the field polarization vector. In the following, we assume the field is polarized linearly along the z axis ($\vec{e}=\vec{e}_z$). Hence,

$$D_L = z_1 + z_2.$$

In this expression, subscripts 1 and 2 refer to the electrons. H is the atomic Hamiltonian (we consider here a two-active-electron atom). The function $F(\tau)$ is given by

$$F(\tau) = \sin(\omega_0\tau+\varphi)\zeta(\tau), \quad -T/2 \leqslant \tau \leqslant T/2,$$

where ω_0 is the average carrier frequency and T is the pulse duration given by $T = n2\pi/\omega_0$ ($2\pi/\omega_0$ is the duration of one optical cycle). The envelope function $\zeta(\tau)$ is supposed to be smooth and equal to zero for $|\tau| > T/2$, as usual. In the present case, the envelope has a cosine-squared shape.

Within the context of ultrashort pulses, we can make further approximations. First, we assume that the resonance condition $E_f - E_i \approx 2\omega_0$ (energy conservation) is fulfilled. We write

$$\begin{aligned}&\langle f|D_L e^{-i(\tau_2-\tau_1)H} D_L|i\rangle \\ &= e^{-i(\tau_2-\tau_1)E_r} \langle f|D_L e^{-i(\tau_2-\tau_1)(H-E_r)} D_L|i\rangle \\ &= \sum_k e^{-i(\tau_2-\tau_1)E_r} \langle f|D_L|k\rangle\langle k|e^{-i(\tau_2-\tau_1)(E_k-E_r)} D_L|i\rangle, \end{aligned} \quad (2)$$

with $E_r - E_i = \omega_0$; $|k\rangle$, $|f\rangle$, and $|i\rangle$ are eigenstates of H, with eigenvalues E_k, E_f, and E_i, respectively. We can now rewrite Eq. (1) as follows:

$$A_{fi}^{(2)} = -\mathcal{E}_0^2 \int_{-\infty}^{\infty} d\tau_2 \int_{-\infty}^{\infty} d\tau_1\, F(\tau_2) e^{iE_f\tau_2} \theta(\tau_2-\tau_1) F(\tau_1) e^{-iE_i\tau_1} \times \sum_k e^{-i(\tau_2-\tau_1)E_r} \langle f|D_L|k\rangle\langle k|e^{-i(\tau_2-\tau_1)(E_k-E_r)} D_L|i\rangle. \quad (3)$$

Our assumption is that, for ultrashort pulse durations, the contribution of intermediate states $|k\rangle$ with $T|E_k - E_r| \ll 1$ dominates. Therefore, since $|\tau_2 - \tau_1| < T$, we write

$$|(\tau_2 - \tau_1)(E_k - E_r)| < T|E_k - E_r| = \frac{2\pi n|E_k - E_r|}{\omega_0} \ll 1.$$

Replacing E_r by $E_i + \omega_0$ in the above inequality, it is clear that the above assumption is valid provided the intermediate states $|k\rangle$ with $|E_k - E_i| \ll \omega_0$ do not contribute in Eq. (3). Consequently, $e^{-i(\tau_2-\tau_1)(E_k-E_r)}$ can be replaced by 1 in expression (3).

Using this closure relation, the two-photon transition matrix amplitude can be written as

$$\begin{aligned} A_{fi}^{(2)} &\approx -\mathcal{E}_0^2 \int_{-\infty}^{\infty} d\tau_2 \int_{-\infty}^{\infty} d\tau_1 \; F(\tau_2) e^{iE_f\tau_2} \theta(\tau_2 - \tau_1) \\ &\quad \times F(\tau_1) e^{-i(E_i - E_r)\tau_1} \langle f|D_L^2|i\rangle \\ &= K(\mathcal{E}_0, \omega_0, \varphi, E_i, E_r, E_f) \langle f|D_L^2|i\rangle. \end{aligned} \tag{4}$$

Physically the latter approximation means that, for ultrashort pulse durations, one photon is absorbed from the ground state, populating with equal probability a large band of intermediate single continuum states, while the remaining bound electron absorbs a second photon, populating the double continuum. We recall that we have assumed the resonance condition $E_f - E_i \approx 2\omega_0$. Far from this region, the above assumption is not valid, but this latter case is less interesting since the two-photon transition matrix element is small.

III. COMPUTATIONAL APPROACH

Keeping in mind the context of ultrashort pulse durations discussed in the preceding section, we calculate the term $\langle f|D_L^2|i\rangle = \langle f|(z_1 + z_2)^2|i\rangle$ [see Eq. (4)]. First, we evaluate the matrix element:

$$A_{12} = \langle \Psi^-(\vec{p}_1, \vec{p}_2)|z_1 z_2|\Phi_0\rangle, \tag{5}$$

where $\vec{p}_i$ is the momentum vector associated with electron i. In the following, $\vec{p}_i$ is characterized by its norm p_i and by its polar and azimuthal angles θ_i and ϕ_i, respectively. We use a correlated wave function [16] for the initial state and three two-body Coulomb wave functions (3C) for the final state [17]:

$$\begin{aligned} \Phi_0(\vec{r}_1, \vec{r}_2) &= \sum_j D_j (e^{-a_j r_1 - b_j r_2} + e^{-a_j r_2 - b_j r_1}) e^{-\gamma_j r_{12}}, \\ \vec{r}_{12} &= \vec{r}_1 - \vec{r}_2, \end{aligned} \tag{6}$$

$$\begin{aligned} &\Psi_{3C}^{-*}(\vec{p}_1, \vec{p}_2; \vec{r}_1, \vec{r}_2) \\ &\quad = e^{i\vec{p}_{12}\cdot\vec{r}_{12}} \varphi_1^{-*}(\vec{p}_1, \vec{r}_1) \varphi_2^{-*}(\vec{p}_2, \vec{r}_2) \varphi_{12}^{-*}(\vec{p}_{12}, \vec{r}_{12}), \end{aligned} \tag{7}$$

where

$$\varphi_x^{-*}(\vec{p}_x, \vec{r}_x) = R(\xi_x) e^{-i\vec{p}_x\cdot\vec{r}_x} {}_1F_1(-i\xi_x, 1; i(p_x r_x + \vec{p}_x \cdot \vec{r}_x)),$$

is a Coulomb wave function with the Sommerfeld parameter ξ_x and

$$\begin{aligned} \vec{p}_{12} &= \frac{1}{2}(\vec{p}_1 - \vec{p}_2), \quad \xi_{12} = \frac{1}{2p_{12}}, \\ \xi_i &= -\frac{Z}{p_i} \quad (i = 1,2), \quad Z = 2, \\ R(\xi) &= e^{-\pi\xi/2}\, \Gamma(1 + i\xi). \end{aligned}$$

In order to calculate the matrix element (5), it is convenient to use the following analytical formula:

$$\begin{aligned} I_x(\vec{p}_x, \vec{A}; \lambda) &= \int \frac{d^3r}{r} e^{-\lambda r} \varphi_x^{-*}(\vec{p}_x, \vec{r}) e^{i\vec{A}\cdot\vec{r}} \\ &= 4\pi R(\xi_x) \frac{[(\lambda - ip_x)^2 + A^2]^{i\xi_x}}{[(\vec{A} - \vec{p}_x)^2 + \lambda^2]^{(1+i\xi_x)}}. \end{aligned} \tag{8}$$

We denote

$$g^*(\vec{p}_{12}, \vec{p}; \gamma_j) = \int d^3 r_{12} e^{-\gamma_j r_{12}} \varphi_{12}^{-*}(\vec{p}_{12}, \vec{r}_{12})\, e^{i(\vec{p} + \vec{p}_{12})\cdot\vec{r}_{12}} \tag{9}$$

and rewrite Eq. (5) in the following way:

$$\begin{aligned} A_{12} = \sum_j D_j \int \frac{d^3p}{(2\pi)^3} g^*(\vec{p}_{12}, \vec{p}; \gamma_j) [G_1(\vec{p}_1, -\vec{p}, \vec{e}; a_j) \\ \times G_2(\vec{p}_2, \vec{p}, \vec{e}; b_j) + (a_j \longleftrightarrow b_j)], \end{aligned} \tag{10}$$

where

$$G_x(\vec{p}_x, \vec{q}, \vec{e}; \lambda) = \int d^3 r e^{i\vec{q}\cdot\vec{r}} \varphi_x^{-*}(\vec{p}_x, \vec{r})(\vec{e}\cdot\vec{r}) e^{-\lambda r}. \tag{11}$$

According to Eq. (8), we obtain

$$g^*(\vec{p}_{12}, \vec{p}; \gamma_j) = -\frac{\partial}{\partial\gamma_j} I_{12}(\vec{p}_{12}, \vec{p}_{12} + \vec{p}; \gamma_j). \tag{12}$$

The integral (8) can be used to calculate the integral (11). It is done by writing the potential vector $\vec{A} = \vec{q} + \varepsilon\vec{e}$, by expanding the left- and right-hand sides of integral (8) in series in ε, and by comparing the terms of the same degree. We obtain

$$\begin{aligned} &F_x(\vec{p}_x, \vec{q}, \vec{e}; \lambda) \\ &\quad = \int \frac{d^3r}{r} e^{i\vec{q}\cdot\vec{r}} \varphi_x^{-*}(\vec{p}_x, \vec{r})(\vec{e}\cdot\vec{r}) e^{-\lambda r} \\ &\quad = -8\pi i R(\xi_x) \frac{[(\lambda - ip_x)^2 + q^2]^{i\xi_x}}{[(\vec{q} - \vec{p}_x)^2 + \lambda^2]^{(1+i\xi_x)}} \\ &\qquad \times \left[i\xi_x \frac{\vec{e}\cdot\vec{q}}{(\lambda - ip_x)^2 + q^2} - (1 + i\xi_x) \frac{\vec{e}\cdot(\vec{q} - \vec{p}_x)}{(\vec{q} - \vec{p}_x)^2 + \lambda^2} \right]. \end{aligned} \tag{13}$$

Correspondingly,

$$G_x(\vec{p}_x, \vec{q}, \vec{e}; \lambda) = -\frac{\partial}{\partial\lambda} F_x(\vec{p}_x, \vec{q}, \vec{e}; \lambda). \tag{14}$$

Finally we get

$$\begin{aligned} A_{12} = -\sum_j D_j \frac{\partial^3}{\partial a_j \partial b_j \partial \gamma_j} \int \frac{d^3p}{(2\pi)^3} I_{12}(\vec{p}_{12}, \vec{p}_{12} + \vec{p}; \gamma_j) \\ \times [F_1(\vec{p}_1, -\vec{p}, \vec{e}; a_j) F_2(\vec{p}_2, \vec{p}, \vec{e}; b_j) + (a_j \longleftrightarrow b_j)]. \end{aligned} \tag{15}$$

The second step consists of calculating the matrix element

$$A_1 = \langle \Psi^-(\vec{p}_1,\vec{p}_2)|z_1^2|\Phi_0\rangle. \tag{16}$$

For this, we define a new function:

$$S_x(\vec{p}_x,\vec{q},\vec{e};\lambda) = \int \frac{d^3r}{r} e^{i\vec{q}\cdot\vec{r}} \varphi_x^{-*}(\vec{p}_x,\vec{r})(\vec{e}\cdot\vec{r})^2 e^{-\lambda r}. \tag{17}$$

Following the scheme presented above, one easily gets

$$A_1 = -\sum_j D_j \frac{\partial^3}{\partial a_j \partial b_j \partial \gamma_j} \int \frac{d^3p}{(2\pi)^3} I_{12}(\vec{p}_{12},\vec{p}_{12}+\vec{p};\gamma_j) \times [S_1(\vec{p}_1,-\vec{p},\vec{e};a_j) I_2(\vec{p}_2,\vec{p},\vec{e};b_j) + (a_j \longleftrightarrow b_j)]. \tag{18}$$

Analogously,

$$A_2 = -\sum_j D_j \frac{\partial^3}{\partial a_j \partial b_j \partial \gamma_j} \int \frac{d^3p}{(2\pi)^3} I_{12}(\vec{p}_{12},\vec{p}_{12}+\vec{p};\gamma_j) \times [I_1(\vec{p}_1,-\vec{p},\vec{e};a_j) S_2(\vec{p}_2,\vec{p},\vec{e};b_j) + (a_j \longleftrightarrow b_j)]. \tag{19}$$

The differential probability is now expressed as follows [with K given in Eq. (4)]:

$$\frac{d^4W}{dE_1 dE_2 d\Omega_1 d\Omega_2} = \frac{2p_1p_2}{(2\pi)^6}\left|A_{fi}^{(2)}\right|^2 \approx \frac{2p_1p_2}{(2\pi)^6}\,|K|^2|2A_{12} \times (\vec{p}_1,\vec{p}_2) + A_1(\vec{p}_1,\vec{p}_2) + A_2(\vec{p}_1,\vec{p}_2)|^2. \tag{20}$$

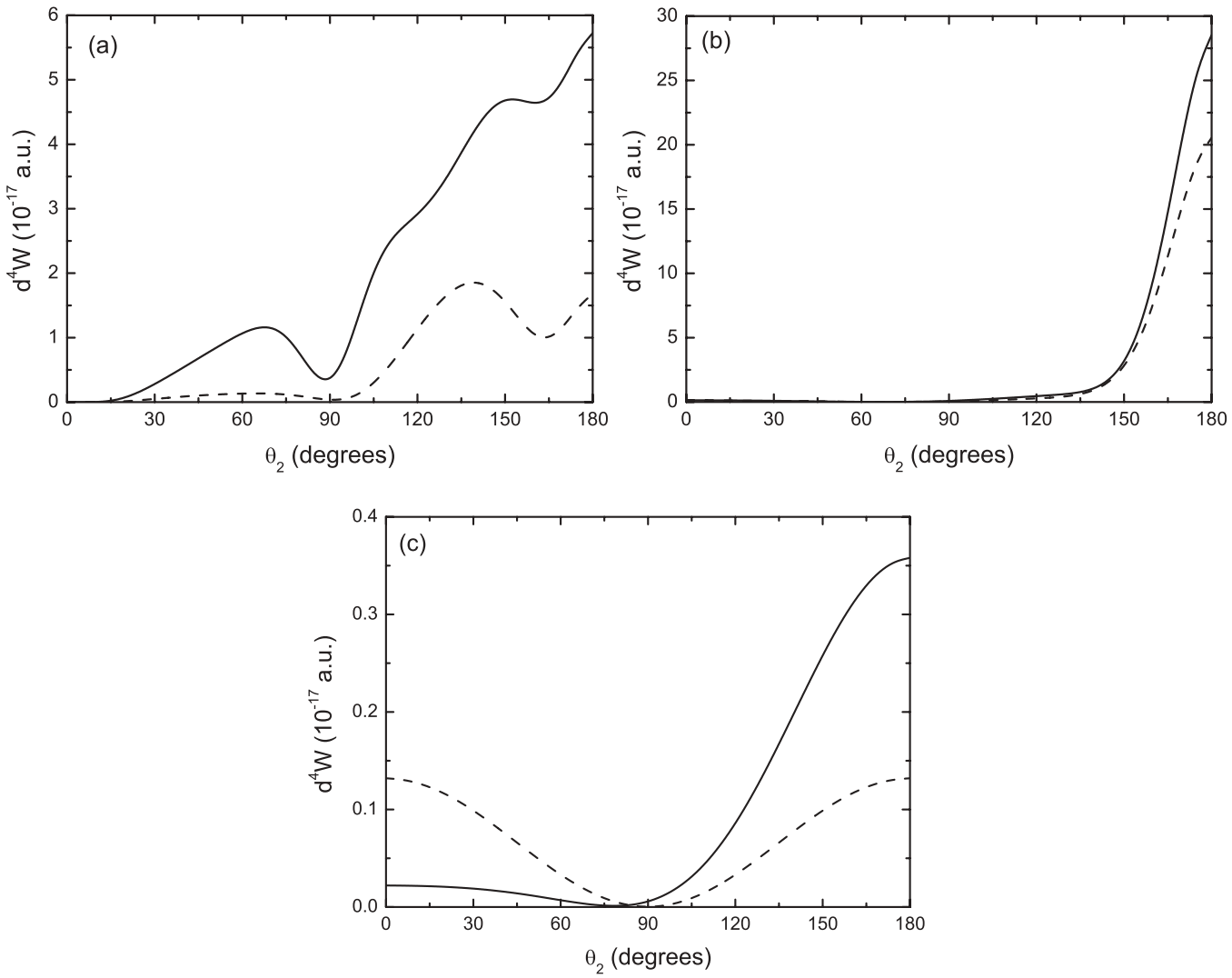

FIG. 1. Differential probability [see Eq. (20)] in a.u. vs the scattering angle θ_2 of the second ejected electron, assuming that the first electron is ejected with a momentum vector $\vec{p}_1$ parallel to the polarization vector $\vec{e}_z$ ($\theta_1 = 0^\circ$). The electron energies in the double continuum are $E_1 = E_2 = 200$ eV. Solid line, results obtained by including all terms in Eq. (20); dashed line, results obtained by neglecting the quadrupole term $A_1 + A_2$ in Eq. (20). (a) The double continuum is described with the 3C wave function and the initial state by a correlated wave function; see Eqs. (6) and (7). (b) The double continuum is described by a simple product of two Coulomb functions and the initial state by a correlated wave function [Eq. (7) with $\xi_{12} = 0$ and Eq. (6)]. (c) The double continuum is a simple product of two Coulomb functions [Eq. (7) with $\xi_{12} = 0$] and the initial state is a product of two screened orbitals [Eq. (22)]. $|K| = 0.0000184$ in Eq. (4).

In order to put the following section in perspective, we now discuss the meaning of the various terms in the above expression. The dipole term A_{12} describes a process in which each electron absorbs one photon. The term $A_1 + A_2$ is a quadrupole term that describes a process in which one electron absorbs two photons and ejects the other electron by collision. Therefore, expression (20) shows clearly that, in the present regime of ultrashort pulse durations, both processes can be disentangled. It also shows that in this very-high-frequency regime, the double ejection mechanism is not purely sequential. In a purely sequential process, the process in which one electron absorbs two photons does not take place. In fact, for ultrashort pulse durations, we are in a transient regime where the distinction between purely direct and sequential processes loses its meaning [18]. In the next section, we use expression (20) to calculate and to study the electron angular and energy distributions as a function of the amount of electron correlations included in the initial and/or final states. The results, which are also compared to a TDSE calculation, shed light on the actual role of the electron correlations.

IV. RESULTS AND DISCUSSION

We start by analyzing how electron correlations in the initial and final states influence the electron angular distributions calculated by means of Eq. (20). We recall that we consider a total pulse duration of two optical cycles, with an intensity of 10^{13} W/cm^2. The values of K [see Eqs. (4) and (20)] are indicated in the figure captions. Figures 1(a), 2(a), and 3(a) give the results of our calculations with electron correlations treated fully in both the initial and the final states for various pairs of electron energy. Figure 1(a) corresponds to $E_1 = E_2 =$ 200 eV, Fig. 2(a) to $E_1 = E_2 = 100$ eV, and Fig. 3(a) to $E_1 = E_2 = 50$ eV. In all cases, we consider a coplanar geometry ($\phi_1 = \phi_2$) where one of the electrons (say electron 1) moves along the polarization direction (i.e., $\theta_1 = 0$) while the other electron is emitted at an angle θ_2. The solid curves are the results given by expression (20), while the dashed ones are obtained by neglecting the quadrupole contribution, namely $A_1(\vec{p}_1, \vec{p}_2) + A_2(\vec{p}_1, \vec{p}_2)$ in Eq. (20).

These results show that the probability with all terms included in Eq. (20) is noticeably bigger than that without

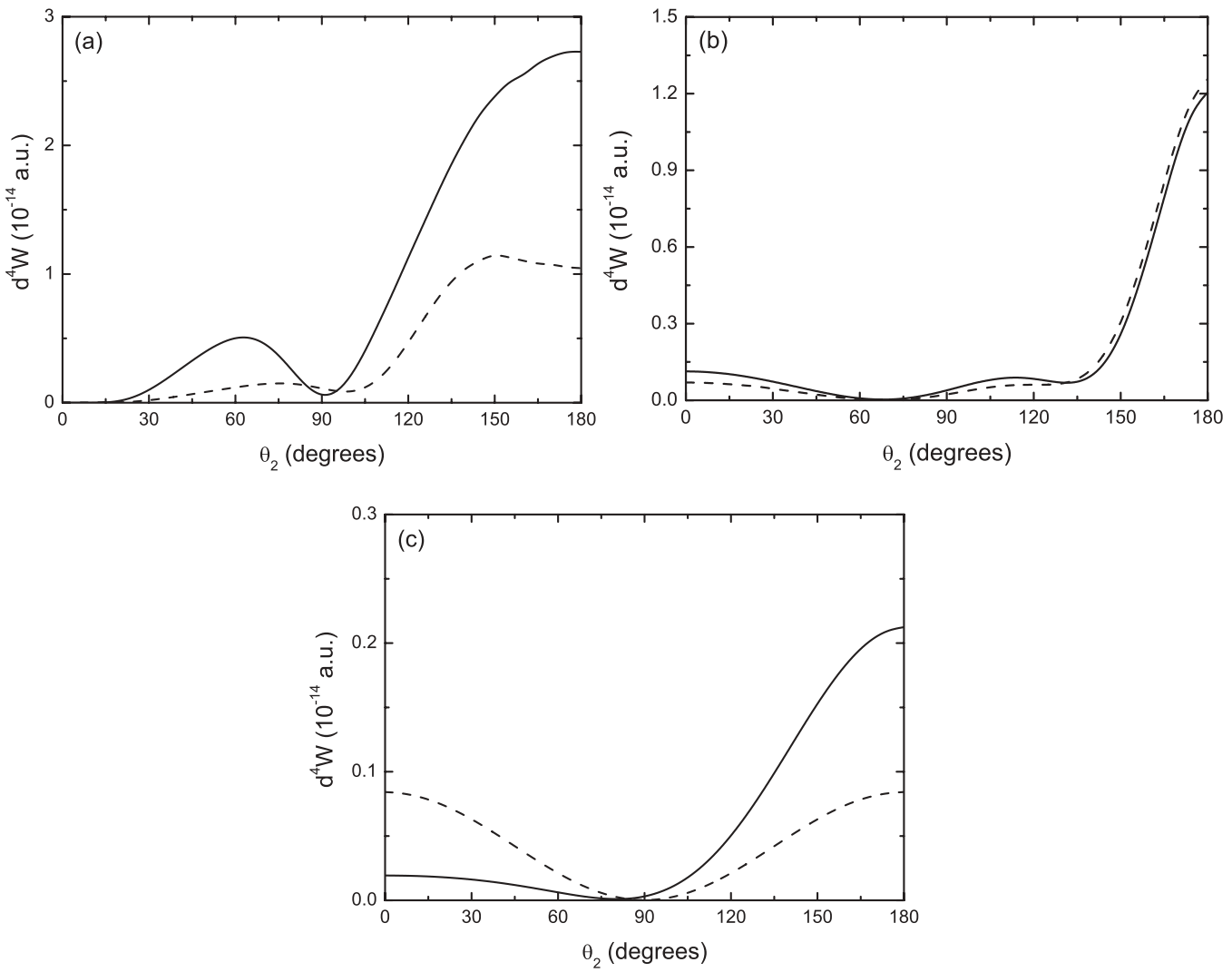

FIG. 2. The same as in Fig. 1, but $E_1 = E_2 = 100$ eV; $|K| = 0.0000542$ in Eq. (4).

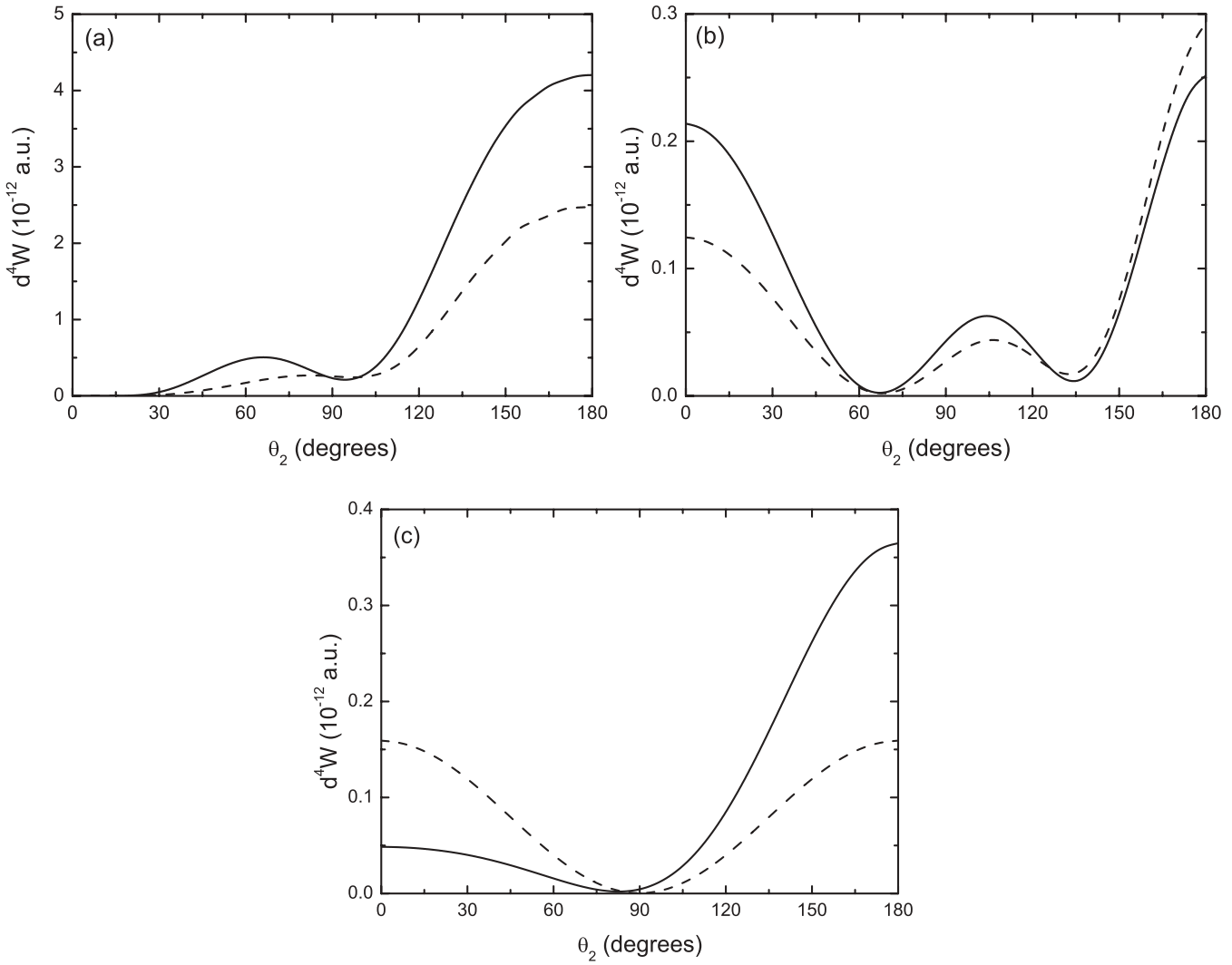

FIG. 3. The same as in Fig. 1, but $E_1 = E_2 = 50$ eV; $|K| = 0.000132$ in Eq. (4).

the quadrupole interactions, and the difference decreases as the total energy $E_1 + E_2$ also decreases. We also observe a local minimum around $\theta_2 = 90^\circ$. In fact, fully neglecting the electron correlations would give a zero at 90° [19]. With electron correlations in the initial and/or final states, the zero is transformed into a minimum around $\theta_2 = 90^\circ$. The deep minimum at small angles $\theta_2 \sim \theta_1$ results from the presence of the so-called Gamov factor $R(\xi_{12})$ in function (7); $|R|^2$ is exponentially small when $\vec{p}_2 \to \vec{p}_1$.

In Figs. 1(b), 2(b), and 3(b), we present results of the fully differential probability where only the ground helium wave function is correlated, whereas the final state is the product of two Coulomb wave functions. We consider the same geometry and the same energy distributions as in the previous case. The results are rather similar to the previous ones, although the different curves exhibit a more complicated structure. The minimum about $\theta_2 = 65^\circ$, which is well visible at all selected energies, becomes more pronounced as the electron energies decrease. Similarly, the maximum around $\theta_2 = 105^\circ$ becomes more marked with decreasing electron energies.

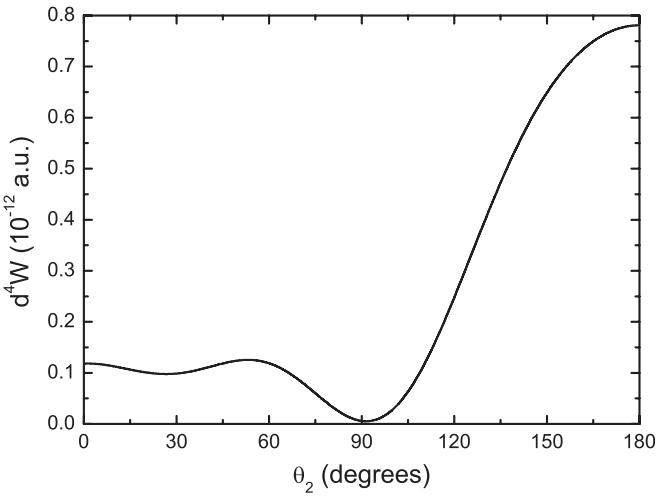

FIG. 4. Differential probability (in a.u.) calculated by resolving the TDSE from $-T/2$, the initial time of the laser pulse, to $t > T/2$, that is, after propagation of the free wave packet (see text). The kinematical conditions are the same as in Fig. 3.

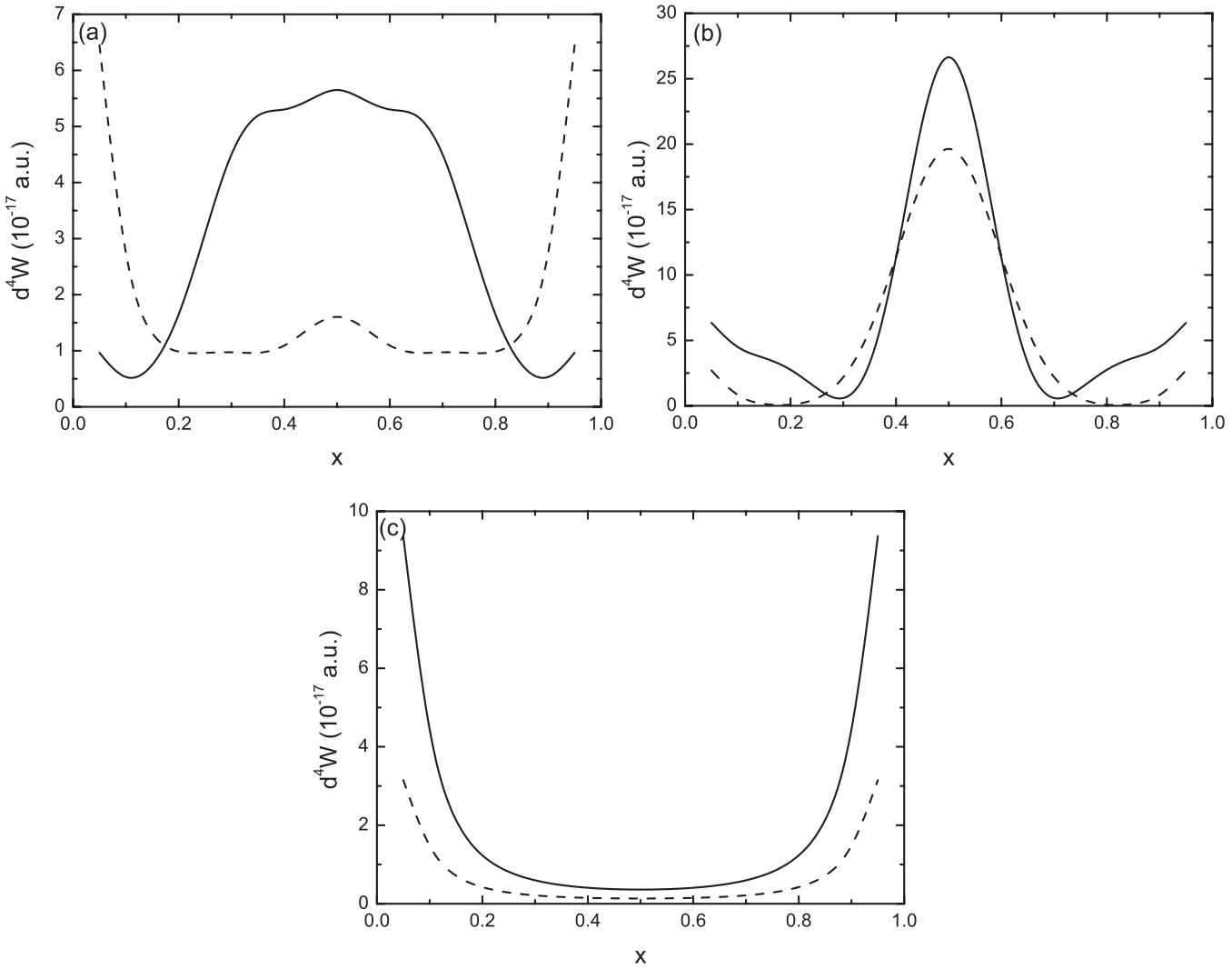

FIG. 5. Differential probability [see Eq. (20)] in a.u. vs the energy sharing variable x (see text). The angles are $\theta_1 = 0^\circ$, $\theta_2 = 180^\circ$; $E = E_1 + E_2 = 400$ eV. Solid line, results obtained by including all terms in Eq. (20); dashed line, results obtained by neglecting the quadrupole term $A_1 + A_2$ in Eq. (20). (a)–(c) Various choices of both the initial and final states as in Fig. 1.

In all the cases considered above, the presence or absence of the quadrupole terms does not affect the positions of maxima and minima. In general, the differential probability may be written as a combination of Legendre polynomials:

$$d^4W \sim |\tilde{c} + \tilde{a}\,P_1(\cos\theta_2) + \tilde{b}\,P_2(\cos\theta_2)|^2. \tag{21}$$

Note that $P_1(\cos\theta_2) = 0$ at $\theta_2 = 90^\circ$, and $P_2(\cos\theta_2) = 0$ at $\theta_2 = 54.7^\circ$ and 125.3°. As explained below, this may lead to new selection rules.

Finally, Figs. 1(c), 2(c), and 3(c) present results for the fully differential probability d^4W for the same geometry and the same electron energies as before. In this case, both electrons are nearly independent and the shapes of all curves do not depend on the energies of the outgoing electrons. Here,

$$\Phi_0(r_1,r_2) = \varphi_0(r_1)\varphi_0(r_2), \quad \varphi_0(r) = \sqrt{\frac{Z^3}{\pi}}e^{-Zr}, \quad Z = 27/16, \tag{22}$$

and the final state is a product of two Coulomb waves. In this particular case of a symmetric distribution of electron energies, we have

$$\begin{aligned} A_{12} &= \langle\varphi^-(\vec{p}_1)|z_1|\varphi_0\rangle\langle\varphi^-(\vec{p}_2)|z_2|\varphi_0\rangle \\ &= a\,P_1(\cos\theta_1)P_1(\cos\theta_2), \end{aligned} \tag{23}$$

$$A_1 = \langle\varphi^-(\vec{p}_1)|z_1^2|\varphi_0\rangle\langle\varphi^-(\vec{p}_2)|\varphi_0\rangle = c + b\,P_2(\cos\theta_1), \tag{24}$$

$$A_2 = \langle\varphi^-(\vec{p}_2)|z_2^2|\varphi_0\rangle\langle\varphi^-(\vec{p}_1)|\varphi_0\rangle = c + b\,P_2(\cos\theta_2). \tag{25}$$

The terms A_1 and A_2 should be zero if the electronic correlations in the initial state are fully absent: $\langle\varphi^-(\vec{p}_i)|\varphi_0\rangle = 0$, or $c = b = 0$ in Eqs. (24) and (25). Taking into account the fact that $\theta_1 = 0$ and inserting Eqs. (23)–(25) into Eq. (20), we obtain

$$d^4W \sim |(2c + b) + 2a\,P_1(\cos\theta_2) + b\,P_2(\cos\theta_2)|^2. \tag{26}$$

At $\theta_2 = 90^\circ$, $P_1(\cos\theta_2) = 0$, the dashed curve reaches zero, and the solid curve is also close to zero. This means that

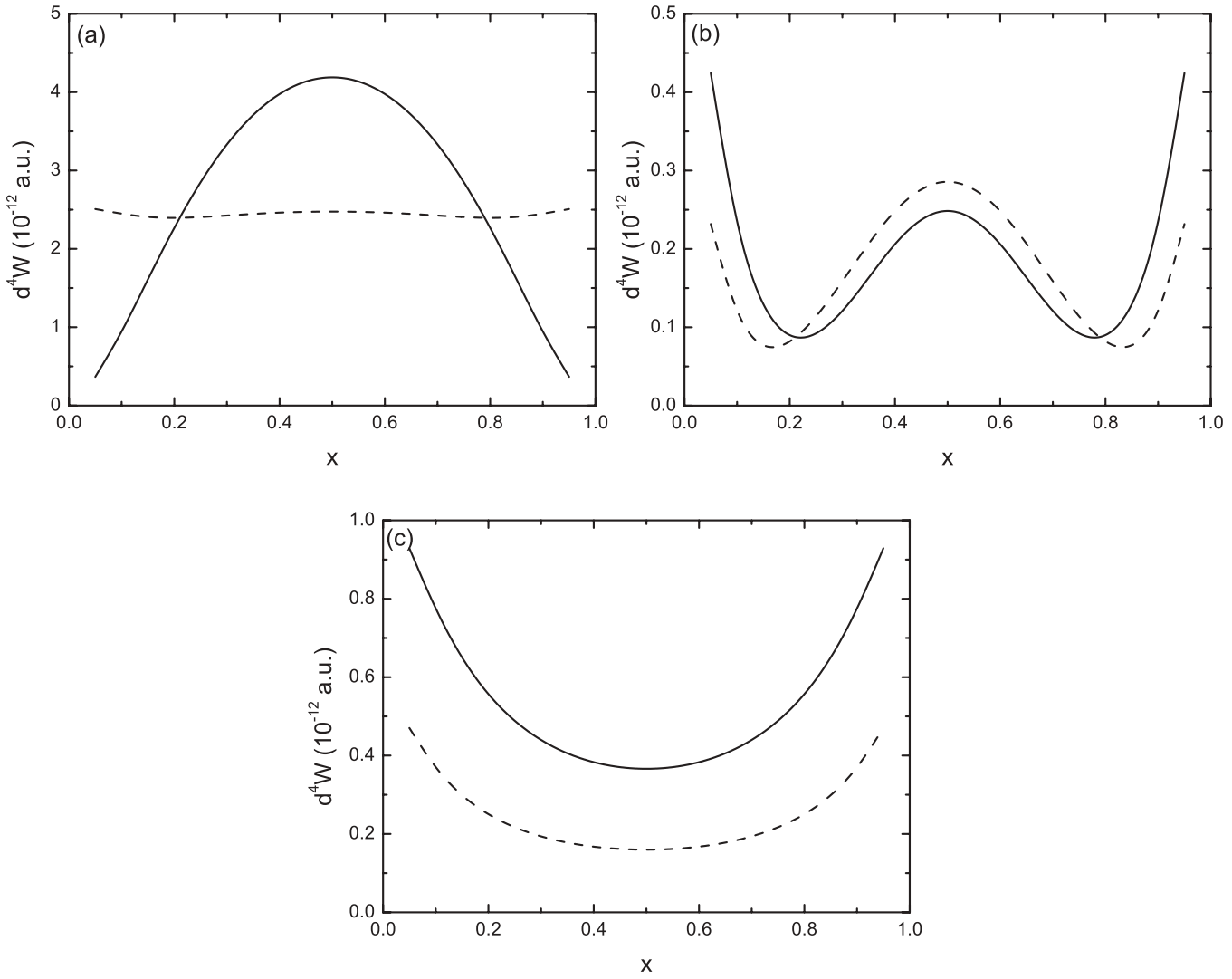

FIG. 6. The same as in Fig. 5, but $E = E_1 + E_2 = 100$ eV.

$2c + b/2 \approx 0$. Considering the behavior of $d^4W(\theta_2)$ for $\theta_2 = 0^\circ$ and $\theta_2 = 180^\circ$, we have

$$\frac{d^4W(180^\circ) - d^4W(0)}{d^4W(180^\circ) + d^4W(0)} \approx -\frac{2\mathrm{Re}\zeta}{1+|\zeta|^2}, \quad \zeta = \frac{5}{4}\frac{b}{a}. \tag{27}$$

Equation (27) shows that b and c are not small any more in comparison with a; instead they are quite comparable. Therefore, even "weak electron correlations" like those taken into account within the mean-field Hartree-Fock approximation for the ground state play a rather important role. When electron correlations are taken fully into account in both the initial and final states, the expression of the amplitude in terms of Legendre polynomials becomes much more complicated. However, our results show that it is essentially the interplay between the various terms that determines the general structure of peaks and dips of the differential probability.

Regarding now the case of 100 eV excess energy ($E_1 = E_2 = 50$ eV), it is interesting to compare our results with the distributions calculated by resolving the TDSE. The method has been described in numerous papers and here we give only a very brief description. We solve the TDSE using a spectral method, the wave functions being developed onto a set of B splines [18,19] defined in a "box" of given radial length. After propagating the initial wave packet until the interaction with the pulse has ceased, we are left with the task of calculating the probability of double ionization. In our approach we use a simple projection of the wave packet onto a product of Coulomb functions at $t > T/2$, that is, at a time where electron interaction in double continuum is weak [14]. It is worth noting that the wave packet should not reach the limit of the box, making the TDSE difficult to apply for high-energy photons. Regarding the problem of propagation, one can formulate it in the context of second-order perturbation theory. First we write

$$\tilde{A}^{(2)}_{fi}(t) = \sum_k \langle \tilde{f}|k\rangle e^{i(E_f - E_k)(t-T/2)} A^{(2)}_{ki}(T/2), \quad t > T/2, \tag{28}$$

with $A^{(2)}_{ki}(T/2)$ given by Eq. (1). If $|\tilde{f}\rangle = |f\rangle$ (i.e., $|\tilde{f}\rangle$ is an eigenstate of H with appropriate asymptotic conditions), it is easy to show that $|\tilde{A}^{(2)}_{fi}(t > T/2)| = |A^{(2)}_{fi}(T/2)|$. If $|\tilde{f}\rangle$ is only an approximate solution (e.g., $|\tilde{f}\rangle$ is an eigenstate of

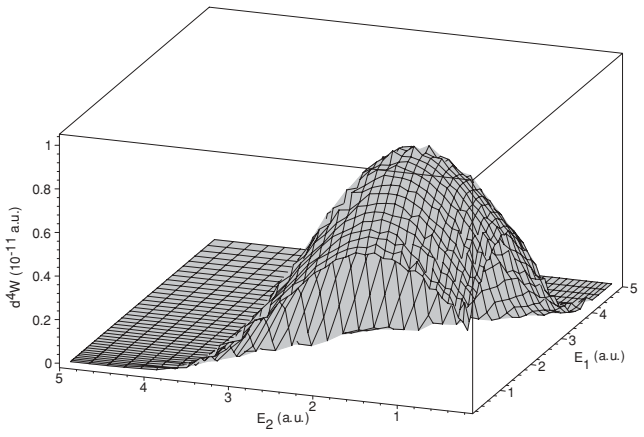

FIG. 7. Three-dimensional energy distributions: result from TDSE calculations. The contribution of the dominant channel ($L = 2$ with $l_1 = l_2 = 1$) is shown.

$\widetilde{H} = H - V$), in general $|\tilde{A}^{(2)}_{fi}(t > T/2)| \neq |A^{(2)}_{fi}(T/2)|$. As a matter of fact, depending on the properties of V (in particular its asymptotic behavior), $|\tilde{A}^{(2)}_{fi}(t > T/2)|$ may be close to $|A^{(2)}_{fi}(T/2)|$. This point is discussed in detail in [20] in the context of single and double ionization. Although the question of extracting TPDI probabilities from TDSE calculations is still open [19], here we consider that (most of the) electron interactions in the double continuum have vanished at t (i.e., the time where the projection onto Coulomb functions is performed). Therefore, the present TDSE calculations should include (most of the) electron correlations in all channels. We return to this point in the following.

In Fig. 4, we present the fully differential probability d^4W for the same kinematical conditions as in Fig. 3 and calculated by solving numerically the TDSE. We note an overall agreement with Figs. 3(a) and 3(c), as far as the shape and the order of magnitude are concerned. A closer examination shows that the minimum and maximum (around $\theta_2 = 60°,90°$) in Fig. 3(a) are in better agreement with the results given in Fig. 4. This is expected since these figures refer to calculations including electron correlations in both initial and final states. Nevertheless, in contrast with Fig. 3(a), TDSE calculation shows a nonzero TPDI differential probability at $\theta_2 = 0°$. According to the above discussion, one expects that TDSE calculations have not converged in the latter region, where electron correlations are strong (the electrons are both emitted in the forward direction with equal velocities). TDSE calculations should be performed in a much larger box to allow the propagation of the wave packet for a long time after the pulse end. Figure 3(b) shows a strong emission in the forward direction, which is unphysical when both electrons have equal energy.

Let us now turn to the energy distributions of the electrons. In Figs. 5 and 6, d^4W is presented versus a variable x, where $E_1 = Ex$, $E_2 = E(1 - x)$ with $0 \leqslant x \leqslant 1$. Here we keep $\theta_1 = 0°$, $\theta_2 = 180°$ which corresponds to a back-to-back electron emission. In Figs. 5(a), 5(b), and 5(c), the energy distribution is given for 400 eV total energy of the two electrons. Figures 6(a), 6(b), and 6(c) correspond to a total energy of 100 eV. For Figs. 5 and 6, we use approximations for the initial and final states similar to those in Figs. 1, 2, and 3. Note that

$$\frac{d^4W}{dE_1\,dE_2\,d\Omega_1\,d\Omega_2} = \frac{d^4W}{E\,dE\,dx\,d\Omega_1\,d\Omega_2}.$$

In all figures, we see again a noticeable contribution of the quadrupole terms $A_1 + A_2$. In Figs. 5(b) and 6(b), the local maximum is reached at $x = 0.5$, whereas in Figs. 5(c) and 6(c) we see a minimum instead. Remember that the amplitudes in both these cases differ only by trial helium wave functions. Figures 5(a) and 6(a) are also rather different from Figs. 5(b) and 6(b). This leads to a first conclusion, namely that possible energy-sharing experiments can supply us with valuable information both on the initial state of the quantum system and on the mechanisms of its interaction with the strong laser pulse. The comparison of Figs. 5(a), 5(b), and 5(c) clearly indicates that the electron correlations in both initial and final states play a crucial role. In the case of nearly independent electrons, the energy distribution exhibits a pronounced U shape, meaning that both electrons are ejected with very different energies. This is in complete contradiction with the results (inverse U shape) obtained when electron correlations are taken into account either in the initial state or in both the initial and final states. Let us note that, within the time-dependent perturbation theory, both the initial and the final states should be eigenstates of the atomic Hamiltonian. In the case of the final state, the correlated 3C wave function has the correct asymptotic behavior but only approximately describes electron correlations in the region where both electrons are still at short distances from the nucleus. The same conclusion about electron correlations can be drawn from Fig. 6. In the case where the total energy of the two ejected electrons is 100 eV, we performed TDSE calculations. They are shown in Fig. 7; in agreement with Fig. 6(a), both electrons tend to be emitted with the same energy. This is a further illustration of electron correlations.

V. CONCLUSIONS

In this work, we have investigated two-photon double ionization of helium in the xuv and ultrashort pulse duration regimes. We have calculated angular and energy distributions. In the case of attosecond pulses, it is possible to express the TPDI probabilities with a simple expression. It contains two terms: the first one is related to one-photon absorption by each electron and the other one refers to two-photon absorption by electron 1 or 2 and the other electron being ejected through correlations effects. Under these approximations, the main problem is to express the initial and final stationary states of helium; the representation of double continuum is the main difficulty here. Several models have been employed to represent the initial (ground) and final (double continuum) states of helium. We have investigated situations where the excess energies in the double continuum are 100, 200, and 400 eV, corresponding to photon energies of 3.29, 5.13, and 8.8 a.u., respectively. We have found that, even in the present high-frequency regime, the two processes are important in contrast to a purely sequential double-ejection mechanism where each electron absorbs, independently, a single photon. Furthermore, the inclusion of electron correlations in both the initial and final states leads to a back-to-back electron emission along the polarization axis with clear equipartition of

the energy. These investigations will be pursued in the direction of heavy atoms, where x rays directly ionize the inner electrons.

ACKNOWLEDGMENTS

H.B. and Y.P. thank the Université Catholique de Louvain for hospitality and financial support. Y.P. thanks the Universitié of Bordeaux I for hospitality and financial support. O.C. acknowledges the financial support of the RFBR (Grant No. 08-01-00604) and of the JINR project "Mathematical support of experimental and theoretical studies" (Grant No. 09-6-1060-2005/2010). Work was partially supported by the European COST Action CM0702 (STSM program).

[1] Yu. V. Popov, O. Chuluunbaatar, V. L. Shablov, and K. A. Kouzakov, Phys. Part. Nucl. **41**, 543 (2010).
[2] D. P. Almeida, A. C. Fontes, and C. F. L. Godinho, J. Phys. B **28**, 3335 (1995); J. Lecointre, J. J. Jureta, and P. Defrance, *ibid.* **41**, 095204 (2008).
[3] H. Bethe, Ann. Phys. **5**, 325 (1930); Z. Phys. **76**, 293 (1932); M. Inokuti, Rev. Mod. Phys. **43**, 297 (1971).
[4] P. Defrance, J. J. Jureta, T. Kereselidze, J. Lecointre, and Z. S. Machavariani, J. Phys. B **42**, 025202 (2009).
[5] A. A. Sorokin, S. V. Bobashev, T. Feigl, K. Tiedtke, H. Wabnitz, and M. Richter, Phys. Rev. Lett. **99**, 213002 (2007).
[6] M. G. Makris, P. Lambropoulos, and A. Mihelič, Phys. Rev. Lett. **102**, 033002 (2009).
[7] Ph. Antoine, E. Foumouo, B. Piraux, T. Shimizu, H. Hasegawa, Y. Nabekawa, and K. Midorikawa, Phys. Rev. A **78**, 023415 (2008).
[8] J. Arthur *et al.*, SLAC National Accelerator Laboratory, Report No. SLAC-R-593, 2002 (unpublished), [http://ssrl.slac.stanford.edu/lcls/cdr/].
[9] H. Wabnitz *et al.*, Nature **420**, 482 (2002).
[10] S. Gordienko, A. Pukhov, O. Shorokhov, and T. Baeva, Phys. Rev. Lett. **93**, 115002 (2004).
[11] S. Gordienko, A. Pukhov, O. Shorokhov, and T. Baeva, Phys. Rev. Lett. **94**, 103903 (2005).
[12] H. Bachau and P. Lambropoulos, Phys. Rev. A **44**, R9 (1991).
[13] E. Foumouo, S. Laulan, B. Piraux, and H. Bachau, J. Phys. B **39**, S427 (2006).
[14] H. Bachau, E. Foumouo, Ph. Antoine, B. Piraux, O. Chuluunbaatar, Y. Popov, and R. Shakeshaft, J. Phys.: Conf. Ser. **212**, 012001 (2010).
[15] C. Cohen-Tannoudji, J. Dupont-Roc, and G. Grynberg, *Photons et atomes* (InterEditions/Editions du CNRS, 1987).
[16] O. Chuluunbaatar, I. V. Puzynin, P. S. Vinitsky, Yu. V. Popov, K. A. Kouzakov, and C. Dal Cappello, Phys. Rev. A **74**, 014703 (2006).
[17] M. Brauner, J. S. Briggs, and H. Klar, J. Phys. B **22**, 2265 (1989).
[18] E. Foumouo, Ph. Antoine, H. Bachau, and B. Piraux, New J. Phys. **10**, 025017 (2008).
[19] E. Foumouo, Ph. Antoine, B. Piraux, L. Malegat, H. Bachau, and R. Shakeshaft, J. Phys. B **41**, 051001 (2008).
[20] L. B. Madsen, L. A. A. Nikolopoulos, T. K. Kjeldsen, and J. Fernández, Phys. Rev. A **76**, 063407 (2007).